Int. J. Electrochem. Sci., 6 **(2011)** 1820 - 1834

International Journal of
ELECTROCHEMICAL
SCIENCE
www.electrochemsci.org

A silver Nanoparticle/Poly (8-Anilino-1-Naphthalene Sulphonic Acid) Bioelectrochemical Biosensor System for the Analytical Determination of Ethambutol

Rachel F Ngece[*], *Natasha West, Peter M Ndangili, , Rasaq A Olowu, Avril Williams, Nicolette Hendricks, Stephen Mailu, Priscilla Baker, Emmanuel Iwuoha*

Sensor Laboratory, Chemistry Department, University of the Western Cape, Private Bag X17 Bellville, Cape Town, 7530, South Africa
[*]E-mail: fngece@uwc.ac.za

Received: 15 March 2011 / *Accepted:* 11 May 2011 / *Published:* 1 June 2011

Ethambutol (2*S*, 2′*S*)-2, 2′-(ethane-1, 2-diyldiimino) dibutan-1-ol) is a first-line antitubercular drug effective against actively growing *Mycobacterium tuberculosis.* Resistance of the mycobacterium to ethambutol among tuberculosis (TB) patients results from inadequate or inappropriate dosing of treatment or using low quality medication. It is therefore necessary to develop reliable methods for determining the ethambutol metabolic profile of patients at point of care for proper dosing. Herein an efficient ethambutol bioelectrochemical nanosensor device is illustrated. It consists of cytochrome P450-2E1 (CYP2E1) immobilised on electroactive nanocomposites of poly (8-anilino-1-napthalene sulphonic acid) (PANSA) and silver nanoparticles (AgNPs) stabilized in polyvinylpyrrolidone (PVP). The performance of the ethambutol nanobiosensor (Au/ PANSA/AgNPs /CYP2E1) was interrogated amperometrically. The biosensor gave a dynamic linear range of 2-12 µM, a sensitivity of 1.125µA/µM, detection limit of 0.7 µM and an apparent Michaelis-Menten constant (K_M^{app}) of 1,008 µM. The low detection limit and the dynamic linear range make the nanobiosensor very suitable for the determination of ethambutol in serum.

Keywords: Ethambutol, cytochrome P450-2E1 (CYP2E1), silver nanoparticles, poly (8-anilino-1-napthalene sulphonic acid) (PANSA), Tuberculosis (TB)

1. INTRODUCTION

In recent years, nanostructured materials have received increasing attention due to their wide range of potential applications. Among these materials, composites of conducting polymers and inorganic nanoparticles in particular often exhibit improved physical and chemical properties over their single-component counterparts, and hence their use is highly recommended [1-2]. Metal

nanoparticles, especially gold, silver and copper, have attracted much attention due to their interesting properties and potential applications in technical fields. On the other hand, chemical resistance and surface modification of these metal nanoparticles together with functional polymers are of significant importance, on which many research works have been developed [3- 6]. Furthermore, embedding these metal nanoparticles inside the core of conducting polymers such as polyaniline and polypyrrole has become a popular and interesting aspect of polymer/metal nanocomposites synthesis as a result of the possibilities of the development of materials for chemical sensors, micoelectronic devices and electrocatalysts. This is due to their highly conductive nature of these polymers coupled with their ease of preparation and good stable environment which effectively accommodates the small dimensioned nanoparticles, thus improving specific electronic and catalytic properties. Various approaches have been employed to prepare polymer/metal composites [7-9]. The most popular method involves the electrodepostion of the monomer at electrode surfaces, followed by the electrodeposition of metal nanoparticles from a precursor salt using either a potential cyclic or a pulsed program. Another route of synthesis involves the polymerization of the monomer simultaneously with the formation of the metal nanoparticles using γ-irradiation or ultraviolet irradiation [10-11].

A new challenge in this area has been the manipulation of polymer/metal composites together with biological molecules. This has led to the development of a novel class of modified electrodes in which both the charge transfer and the preservation of biological activity is obtained through experimental techniques designed to manipulate metal nanoparticles and polymers, tissues, DNA fragments, enzymes and other biological molecules. Two main problematic aspects with regards to the development of enzyme-based biosensors are the incorporation of sensing components in suitable matrices and the monitoring of the interaction of these components with analytes. Another aspect in enzymatic devices is the control of enzyme, which is dependent on the interface between the enzyme and polymers/metal composite. Such control has led to immobilization techniques suitable for anchoring the enzyme in close proximity to the electrode surface, thus preserving the biological activity. Therefore, in electrochemical devices where preservation of biological activity at the polymer/metal-enzyme interface is priority towards efficient electrode design, the charge transfer between the enzyme and the electrode is usually fast and reversible [12-15].

Herein we report an efficient enzymatic bioelectrochemical device, in which Cytochrome P450 2E1 was immobilized on electroactive nanostructured composites made from poly (8-anilino-1-napthalene sulphonic acid) and silver nanoparticles and used for the determination of ethambutol; a TB treatment drug. The technique employed here is an improvement from available techniques such as high performance liquid chromatography, thin layer chromatography and gas chromatography used for quantifying the levels of ethambutol and its metabolites in urine and plasma. These are accurate and well established techniques however, generation of results is time consuming and substantial sample preparation is required [16]. These factors pose a problem when dealing with cases of drug resistance and illness arising from severe side effects amongst TB diagnosed patients, making it difficult to monitor the levels of ethambutol in their systems. We therefore present a novel nanobiosensor system for the determination of ethambutol which has reduced sample preparation time and the ability to allow for point of care analysis by studying the biotransformation of the drug in serum.

2. EXPERIMENTAL PART

2.1. Reagents and materials

Analytical grade methanol, silver nitrate ($AgNO_3$) and polyvinylpyrrolidone (PVP) were purchased from Sigma-Aldrich and used for the synthesis of the silver nanoparticles. Electropolymerization was achieved by the use of 8-anilino-1-napthalene sulfonic acid, ammonium hydrate salt 97% (ANSA) (Sigma-Aldrich) in the polymerization medium, sulphuric acid (Fluka). The nanobiosensors were prepared using, Cytochrome P450-2E1 Isozyme (CYP 2E1); EC 1.14.14.1 (Sigma-Aldrich). One unit of CYP2E1 is said to be the required amount to convert 1 picomole of p-nitrophenol to 4-nitrocatechol per minute at a pH of 7.4 and at temperature of 37^0C. The reaction medium, 0.1 M, pH 7.4 phosphate buffer was prepared from dihydrogenorthophosphate dehydrate, anhydrous and disodium hydrogenorthophosphate all purchased from Sigma-Aldrich. The nanobiosensor substrate, ethambutol capsules (2*S*, 2′*S*)-2, 2′-(ethane-1, 2-diyldiimino) dibutan-1-ol) $C_{10}H_{20}N_2O_2$ were supplied by the University of Western Cape Health Centre and were used without further purification dissolved in 0.1 M, pH 7.4 phosphate buffer. De-ionized ultra-filtered water used throughout these experiments was prepared with a Milli-Q water purification system. Analytical grade argon obtained from Afrox, SA was used for degassing the cell solutions. All the solutions were kept refrigerated at 4^0C when not in used.

2.2. Apparatus and measurement

All electrochemical experiments were carried out using a BAS 100W integrated automated electrochemical workstation BioAnalytical Systems (BAS, West Lafayette, IN) controlled by a computer and a conventional three-electrode system with a 0.0201 cm^2 gold (Au) disk as the working electrode, a platinum (Pt) wire auxillary electrode and Ag/AgCl reference electrode with a 3 M NaCl salt bridge solution, all purchased from BAS. All the results obtained using cyclic (CVs), differential pulse (DPV) square wave (SWV) voltammograms and chronoamperometry (constant potential amperometry) were recorded with a computer interfaced to the electrochemical workstation. The working electrode was polished using alumina micropolish and polishing pads (Buehler, IL, USA). Ultraviolet-Visible (UV-Vis) absorbance experiments were performed at room temperature using Nicolet Evolution 100 (Thermo Electron Cooperation) with studies carried out by immobilizing all samples on Indium Tin Oxide (ITO) electrodes.

2.3. Synthesis of silver nanoparticles (AgNPs)

Silver nanoparticles were prepared by a soft solution technique starting with a solution of ($AgNO_3$) and an aqueous solution of PVP. In a typical synthesis; 30 mg $AgNO_3$ was dissolved in 140 mL of methanol and brought to a boil. A second solution was prepared by dissolving 200 mg PVP in hot deionized water and 10 mL of this second solution was then added dropwise to the $AgNO_3$ solution under vigorous stirring. The colour of the mixture became pale red several minutes after methanol

began to boil. Addition of the PVP solution caused the mixture to become increasingly darker until a red-orange colour was reached signifying completion of the silver nanoparticles synthesis. 20 μL of AgNP were drop casted onto Au electrode and allowed to dry for 3hrs after which the Au/PVP-Ag electrode was characterized using CV at the potential window of -300 to +1100 mV at various scan rates in 0.1 M pH 7.4 phosphate buffer.

2.4. Preparation of the Au/PVP-Ag-PANSA/CYP2D6 nanosensor

Electrosynthesis and characterization of PANSA was achieved using the procedure reported by [17]. Modification of the Au electrode was made by casting 10 μL of the silver colloid onto the PANSA film and allowed to dry at room temperature for 3 h after which it was characterized using CV at -300 to +1100 mV at various scan rates in 0.1 M, pH 7.4 phosphate buffer. The PANSA/PVP-AgNPs nanocomposite was then reduced at a constant potential of -600 mV under an argon blanket in a 5 mL solution of buffer until a steady state current was attained which took 5 min to attain. 20 μL of CYP 2E1 was added to the 5 mL solution of buffer, and the Au/ PANSA/PVP-AgNPs /nanocomposite was oxidized at a potential of +700 mV for 20 min during which the PANSA/PVP-Ag nanocomposite was electrostatically attached with CYP 2E1. The resultant Au/PANSA/ PVP-AgNPs /CYP2E1 biosensor was rinsed in buffer and stored refrigerated at -4^0C when not in use. The bioelectrode was polarised at -410 mV where stirring was maintained at 500 rpm during which the background current was allowed to decay to a constant value of approximately 410 s. Chronoamperometric curves were carried out using the biosensor at different concentrations of ethambutol using 0.1 M, pH 7.4 phosphate buffer as the supporting electrolyte. Further studies of the biotransformation of ethambutol were also carried out using CV at a potential window of -800 to +200 mV at 20 mV/s.

3. RESULTS AND DISCUSSION

3.1. Au/PANSA/PVP-AgNPs electrode characterization

Firstly, a film of PANSA was deposited at the Au electrode surface by potentiodynamic oxidative polymerisation. The Au/PANSA electrode was characterised with CV using 0.1 M, pH 7.4 phosphate buffer as the supporting electrolyte. Figure 1A illustrates two redox processes taking place at + 550 and +600 mV labelled a/c and at +220 and +350 mV labelled b/d. The redox process a/c can be attributed to the transformation of aniline in ANSA from the reduced polyleucoemeraldine state to the partly oxidized polyemeraldine state. The redox process b/d is due to the transition of polyleucoemeraldine state to the pernigraniline state, accompanied by oxidation of the ANSA monomer. The voltammograms correspond to a reversible system with $I_{p,a}$ (peak a) / $I_{p,c}$ (peak c) = ~1.1 and $\Delta E_p = E_{p,a}$ (peak a) – $E_{p,c}$ (peak c) < 57/n mV indicating that the polymer behaved as a stable redox species adsorbed on the electrode surface [18-20]. Upon varying the scan rate, ν it was observed that the charge transfer was diffusion controlled up to 50 mV/s with no lack of linearity in the I vs $\nu^{1/2}$ plot

(Results not shown). The Au/PANSA electrode was highly stable, displaying similar electrochemistry after several cycles in the presence of other electrolytes such as nitric acid and hydrochloric acid.

A layer of the AgNPs was deposited by drop-coating on the Au/PANSA electrode after polymerization of PANSA. The effect of the AgNPs on the electroactivity of PANSA was evaluated by comparing the profile of the three electrodes namely; Au/PANSA, Au/PVP-Ag and Au/PANSA/PVP-AgNPs. For the Au/PVP-Ag electrode, a pair of quasi-reversible redox peaks was obtained at +490 and +180 mV resulting from the Ag(0) to Ag(I) transition (Figure 1B) . With increasing scan rate, the AgNPs oxidation peak is seen to be shifted cathodically, from +180 (peak e in Fig. 1B) to +195 mV (peak g in Fig. 1C) and the reduction peak from +490 (peak f in Fig. 1B) to +395 mV (peak h in Fig. 1C).

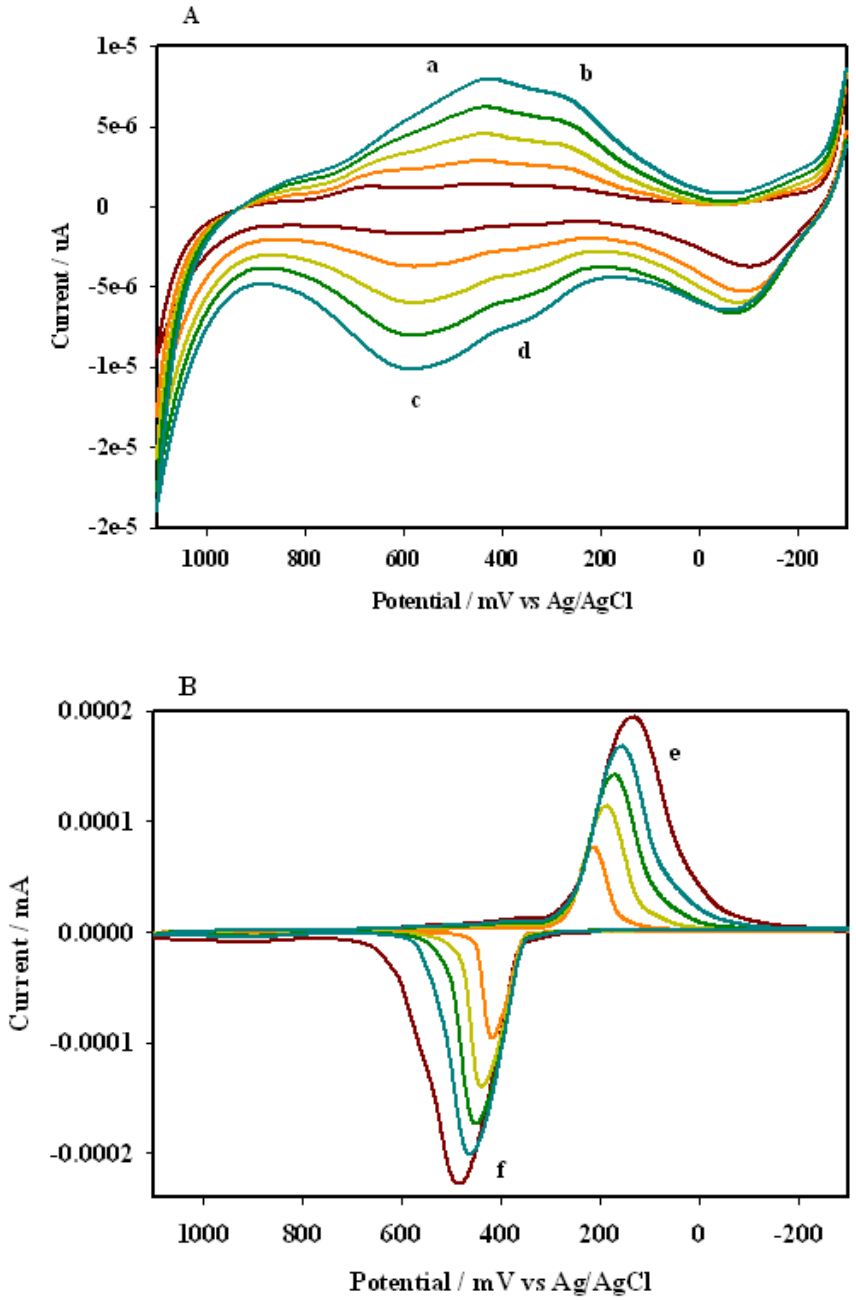

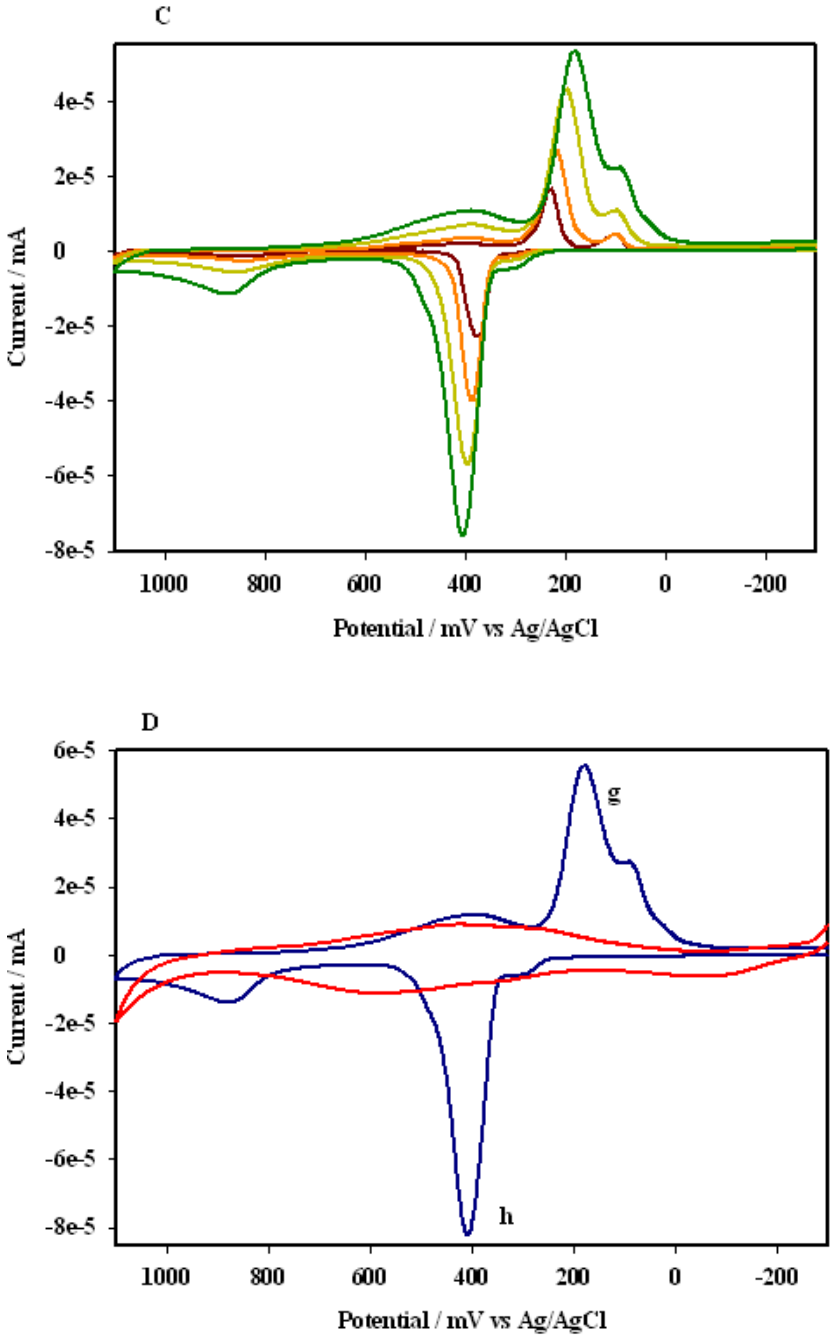

Figure 1. (A) CVs for the synthesis of Au/PANSA. (B) CVs of Au/PVP-AgNP electrodes (C) CVs of Au/PANSA/PVP-Ag at 5, 10, 20, 30, 50 mV/s in 0.1 M, pH 7.4 phosphate buffer and (D) CVs of Au/PANSA (red line) and CVs of Au/PANSA/PVP-AgNP (blue line) electrodes at 50 mV/s in 0.1 M, pH 7.4 phosphate buffer.

Li and co-workers [21] also reported a similar pattern illustrating more negative peaks on glassy carbon electrode. In another study using glassy carbon electrode [22], the oxidation peak was observed at +700 mV and the reduction peak at +330 mV. The shift is accompanied by a large background current, indicating that electroactive area of Au electrode has been increased due to the high special surface area of PVP-AgNPs.

Of great interest is the fact that for the Au/PANSA/PVP-AgNPs electrode, both PANSA (from the Au/PANSA electrode) and AgNPs redox peaks are clearly evident in the voltammograms illustrated in Figure 1D. This gives an indication of the strong interaction between PANSA and PVP-AgNPs. For the Au/PANSA/PVP-AgNPs electrode, the peak current decreased as compared to the Au/PVP-AgNPs electrode. This may be attributed to the further modification of PANSA by PVP-AgNPs on the electrode surface, and the nanocomposite blocked the mass transfer of electroactive probe. The reduced current did not affect the electroactivity of PANSA since there was no significant shift or change in the PANSA peaks as demonstrated by the peak at around +120 mV resulting from the transformation of aniline in ANSA from the reduced polyleucoemeraldine state to the partly oxidized polyemeraldine state [10, 15-21].

3.2. UV-visible spectroscopic analysis

UV-visible spectroscopy is a useful tool for monitoring the possible changes in the Soret absorption band which exists in heme group regions. Band shifts provide information of possible denaturation of heme proteins particularly that of conformational changes. Therefore, in this study this technique was employed to investigate the interaction between CYP2E1 and PANSA/PVP-AgNPs [23-24]. Figure 2 shows the spectra of CYP2E1 in buffer and CYP2E1 immobilized onto PANSA/PVP-AgNPs electrodeposited on ITO electrode. As seen from Figure 2, an absorption peak was observed at 449 nm for pure CYP2E1, while lower peaks at 451 nm for Au/PVP-AgNPs/CYP2E1 and 353 nm for Au/PANSA/PVP-AgNP/CYP2E1. The slight shift of 2 nm in the Soret band may be due to the interaction between CYP2E1 and the PANSA/PVP-AgNP nanocomposite. Such an interaction neither destroyed the protein structure nor changed the fundamental microenvironment of the protein and its conformation.

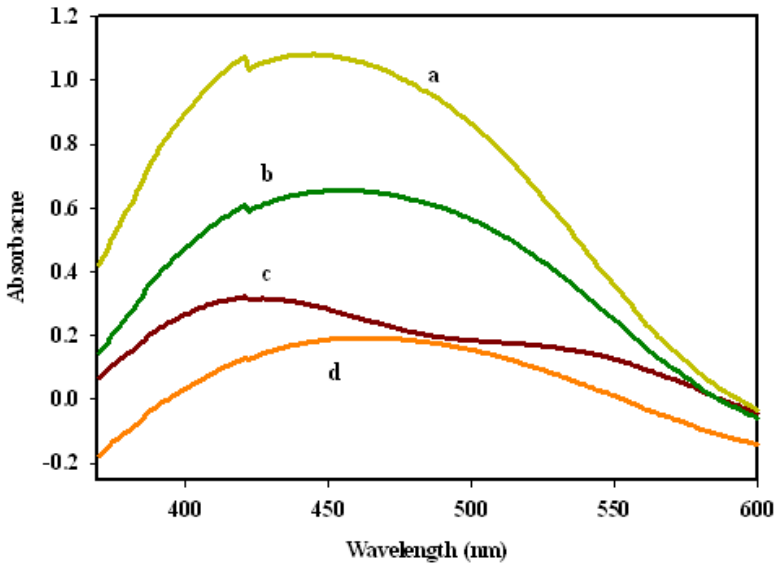

Figure 2. UV- visible spectra of (a) CYP2E1 (b) CYP2E1/PVP-AgNP (c) PANSA/PVP-AgNP composite and (d) PANSA/PVP-AgNP/CYP2E1

This result indicates no observable denaturation of CYP2E1 occurred on the PANSA/PVP-AgNP film. A similar interaction has also been observed by the work carried out by Yu and co-worker; 2010 where haemoglobin was immobilized on colloid silver nanoparticles-chitosan film. The spectrum observed for PANSA/PVP-AgNP illustrates two absorbance peaks at around 425 nm and 535 nm. Although these peaks are shifted from their normal positions, they are as a result of $\pi - \pi^*$ transition. The absence of characteristic peaks attributed to polaron - π^* and π – polaron transitions of PANSA may be related to reaction time. The same behaviour was observed in a study by Jing et al, 2007 [25] involving the synthesis and characterization of Ag/polyaniline core-shell nanocomposites.

3.3. Enzyme modified Au/PANSA/PVP-AgNP bioelectrode

In order to investigate the electrochemical properties of the Au/ PANSA PVP-AgNPs/CYP2E1film, CV of different electrodes in buffer were recorded, as shown in Figure 3. No peaks were observed at bare gold electrode (curve a) while peaks were observed for the PANSA/PVP-AgNPs modified electrode (curve b) and (curve c) obtained after injection of 20 µL CYP2E1 in 0.1 M pH 7.4 phosphate buffer under anaerobic conditions at 20 mV/s. The pair of redox peaks arose from the redox of the heme Fe centre of CYP2E1 embedded in the PANSA/PVP-AgNPs nanocomposite attributed to the (Fe^{2+}/Fe^{3+}) transition [26-27]. Thus, PANSA/PVP-AgNPs must have a great effect on the kinetics of electrode reaction providing a suitable environment for CYP2E1 to transfer electrons with the underlying electrode. It was found that the peak currents of the CYP2E1 enzyme at the PANSA/AgNPs modified electrode were larger than those of at the bare gold electrode with a clear defined redox pair at +790 (oxidation peak) and +150 mV (reduction peak) with the separation of peak potential (ΔE_p) of +640 mV and formal potential (defined as the average of the anodic and cathodic peak potential) of $E^{0'} = E_{p,a} + E_{p,c}/2 = +450$ mV.

Heme proteins exhibit different formal potentials which is attributed to the effect of different system configurations and different microenvironments on the direct electron transfer [10]. Zong et al [28] obtained a formal potential of -36 mV for the direct electron transfer hemogloblin immobilized in multi-walled carbon nanotubes enhanced grafted collagen. On the other hand, Yang et al [29] immobilized myoglobin and gold nanoparticles on a glassy carbon electron by a nafion film, where a pair of reversible redox peaks appeared with a formal potential of -373 mV.

The variation of scan rates (Data not shown) for the Au/ PANSA PVP-AgNPs/CYP2E1 electrode illustrated an increase in the peaks current with increasing scan rates, indicating that the electrochemical behaviour of CYP2E1 immobilized on Au/PANSA/PVP-AgNPs nanocomposite was a surface controlled process. It was also found that the peak potentials varied with an increase in scan rate, while the formal potential was kept almost unchanged, showing that CYP2E1 does not hinder charge transport across the PANSA/PVP-AgNPs film, but enhances electron transportation between the CYP2E1 active site and the electrode surface [30].

According to Laviron equation (Equation1);

$$Ip = n^2F^2A\Gamma^*\nu / 4RT = nFQ\nu / 4RT \qquad (1)$$

Where Γ^* is the electroactive CYP2E1 amount (mol cm^{-2}) and Q is the quantity of charge (C) with the symbols *n, Ip, R, F* and *T* bearing their usual meaning.

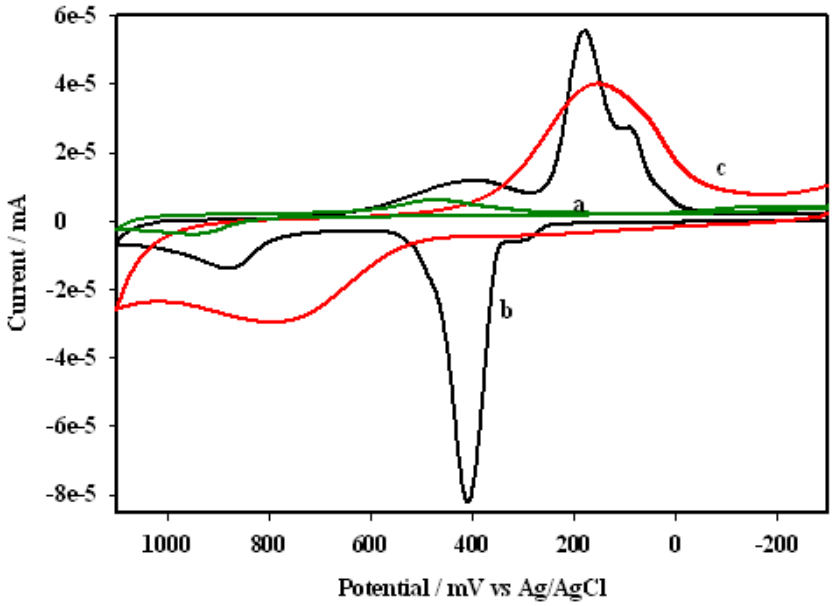

Figure 3. (a) CVs of bare Au electrode (green line) (b) CVs of Au/PANSA/PVP-Ag (black line) and (c) Au/PANSA/PVP-Ag after CYP2E1 immobilization (red line) at 50 mV/s in 0.1 M pH 7. phosphate buffer.

From the slope of $I_{p,c}$ versus ν plot (Data not shown), *n* was calculated to be 1.21 indicating a one electron reaction reaction of CYP2E1 on PANSA/PVP-AgNP. The average coverage of CYP2E1 on the surface of the modified electrode was estimated to be 8.25 x 10^{-5} mol cm^{-2}, 4.56 x 10^{-5} mol cm^{-2} for the Au/PANSA/AgNP electrode. As $\Delta E_p \geq 200$ mV/n the heterogeneous rate constant (ks) can be estimated by Laviron equation.

$$\log ks = \alpha \log(1-\alpha) + (1-\alpha)\log\alpha - \log(RT/nF\nu) - \alpha(1-\alpha)nF\Delta Ep/2.3RT \qquad (2)$$

Taking the electron transfer coefficient α of 0.52, calculated from a plot of E_p versus log ν (Data not shown), a scan rate of 100 mV/s and ΔE_p of +640 mV, the rate constant was estimated to be 1.75 $s^{-1.}$ The estimated value is in the controlled range of the surface-controlled quasi-reversible process, and is in agreement with the values (0.41 s^{-1}, 0.71 s^{-1} and 0.62 s^{-1} respectively) reported by Laviron and co for heme proteins, thus indicating that the active centre (Fe^{3+}/Fe^{2+}) of CYP2D6 underwent a quasi reversible process [31-33].

3.3. Electrochemical behaviour of Au/PANSA/PVP-AgNP/CYP2E1 biosensor

The electrocatalytic activity of CYP2E1 in the PANSA/PVP-AgNPs nanocomposite was evaluated by DPV, CV and chronoamperometric methods. Au/ PANSA/PVP-AgNPs/CYP2E1 was

employed as the working electrode and its electrochemical response towards ethambutol was investigated in 0.1 M, pH 7.4 phosphate buffer under aerobic conditions at 20 mV/s. Figure 4A illustrates the chronoamperometric analysis at different ethambutol concentrations, where the current as a function of time was monitored. The first addition of ethambutol caused an increase in the current and the amperometric response of the sensor was allowed to attain steady state value which took about 20 s to acquire. Using DPV and CV (Figure 4B), a well-defined reduction peak was observed for the Au/PANSA/PVP-AgNPs/CYP2E1 biosensor in deoxygenated buffer. However when ethambutol was injected into the buffer reaction medium, the reduction peak increased with no corresponding oxidation peak observable. With reference to scheme 1, this suggests the one electron electrochemical reduction of the hexa-coordinated low-spin ferric enzyme (Fe^{3+}) to the high spin ferrous enzyme (Fe^{2+}). This form of the enzyme has a high affinity for oxygen and thus binds molecular oxygen present in the solution forming the CYP2E1 (Fe^{2+}) O_2 complex. This interaction results in the development of an aldehyde intermediate followed by the release of a water molecule. The result is a highly active iron-oxoferryl intermediate CYP2E1 (Fe^{4+}) which produces a dicarboxylic acid form of ethambutol upon reduction [34-37].

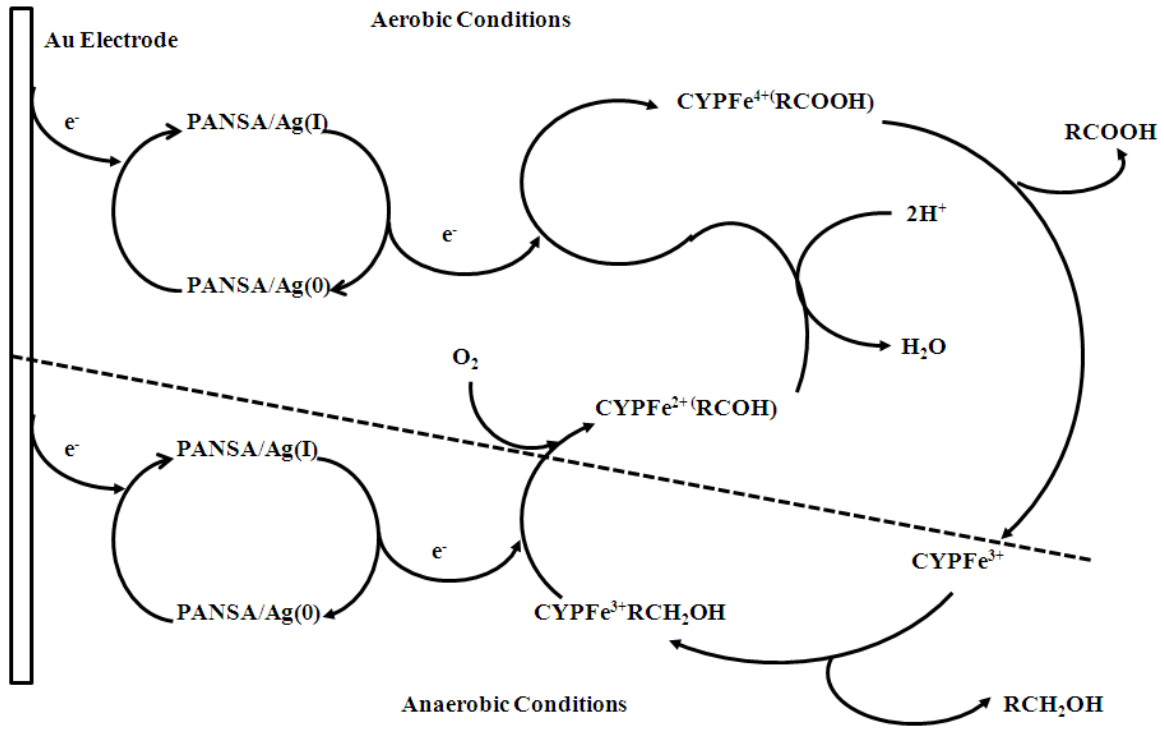

KEY
RCH_2OH – Ethambutol
RCOH – Ethambutol aldehyde intermediate
RCOOH – Dicarboxylic acid
$CYP^{4+, 3+, 2+}$ - Different oxidation states of Cytochrome P450-2E1
PANSA/Ag - silver nanoparticle /poly (8-anilino-1-naphthalene sulphonic acid) nanocomposite

Scheme 1. Reaction scheme for the Au/PANSA/PVP-Ag/CYP2E1 biosensor.

As expected for enzymatic processes, the response upon ethambutol addition led to a Michaelis-Menten profile, with a linear response up to 12 µM and a sensitivity of 1.13 µA/ µM and a detection limit of 0.7 µM (Figure 4C). Thus the Au/PANSA/PVP-AgNPs/CYP2E1 electrode provided a comfortable and friendly environment for the biocatalytic reaction to take place, which was more evident by the determination of the apparent Michaelis-Menten constant (K_M^{app}). The enzymatic reaction at the PANSA/ PVP-Ag electrode surface can be considered as follows:

$$\text{CYP2E1} + \text{Ethambutol} \rightarrow \text{CYP2E1} - \text{Ethambutol} \qquad K_1$$

$$\text{CYP2E1} - \text{Ethambutol} \rightarrow \text{CYP2E1} + \text{Ethambutol Aldehyde} + H_2O \qquad K_2$$

Therefore, based on the Michaelis-Menten reaction, the enzymatic kinetics of CYP2E1 as shown in Equation 3 is written as follows:

$$V = K_2[CYP2E1][ETHAMBUTOL]/K_m + [ETHAMBUTOL] \qquad (3)$$

Where V is the rate, K_2 the equilibrium constant, K_m the Michaelis-Menten constant, [CYP2E1] the concentration of CYP2E1 and [ETHAMBUTOL] is the concentration of ethambutol. Naturally, lower K_m and higher V values are preferred since they indicate a high enzyme biocatalytic activity. These parameters were studied from Figure 4C, where the entire enzymatic reaction is represented by the hyperbolic graph. At lower ethambutol concentrations, the rate of reaction is directly proportional to the ethambutol concentration illustrated in the linear range of Figure 4B. Therefore, when $V = V_{max}$ (the maximum rate), then K_m is numerically equal to half the ethambutol concentration. The value of K_m was therefore determined and found to be 6.30 µM [38-40].

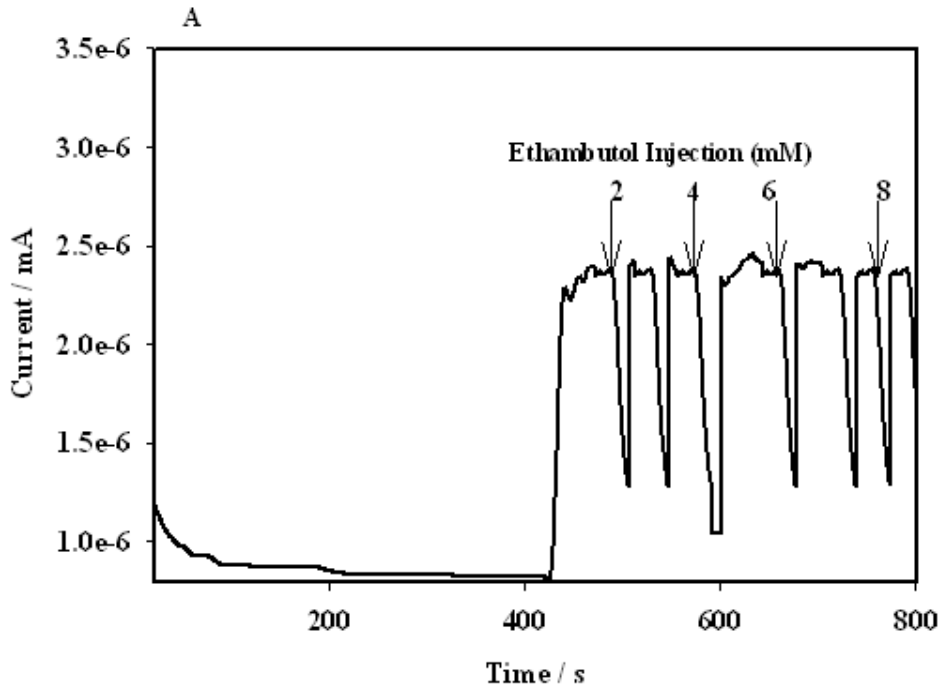

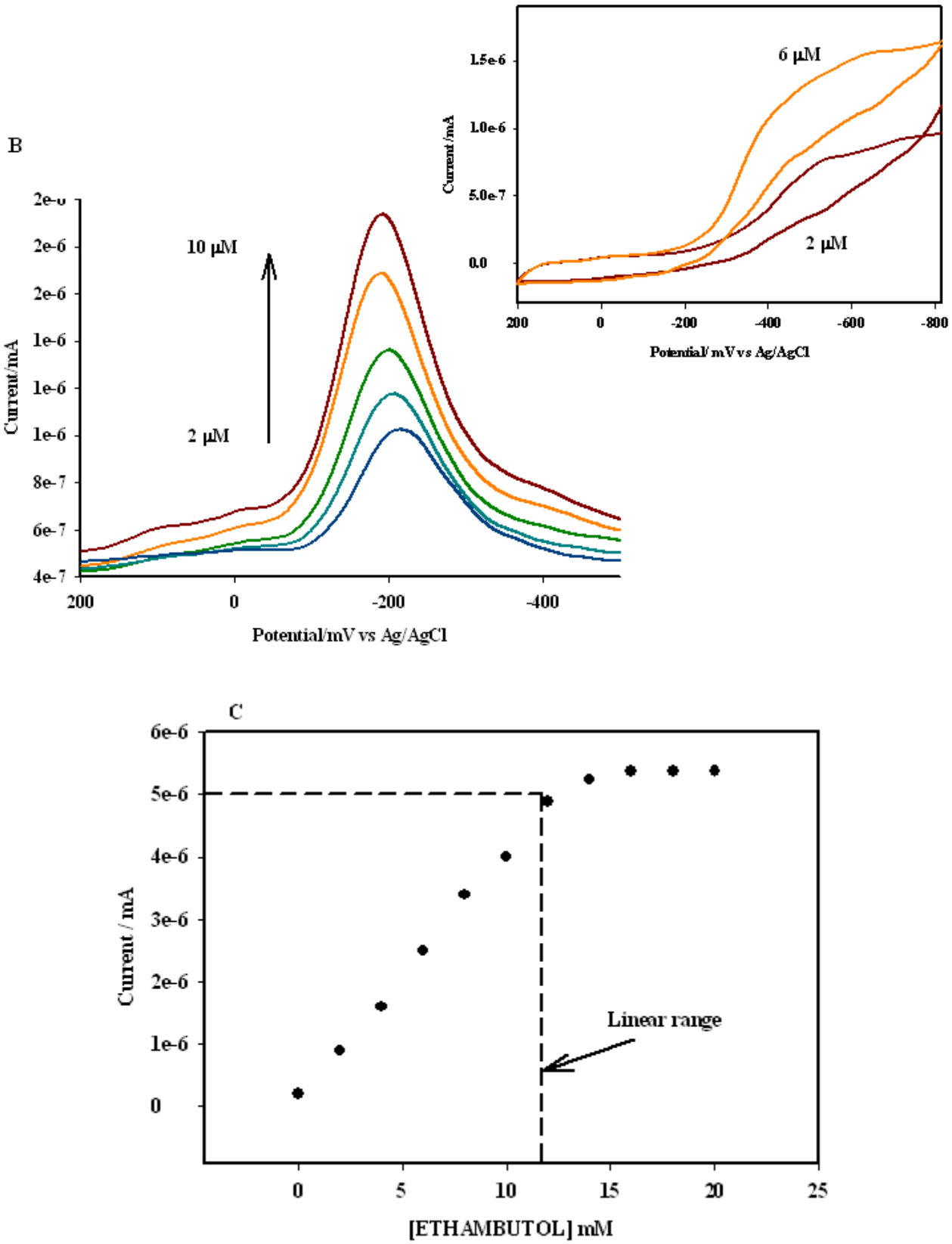

Figure 4 (A) Chronoamperometric curves at applied potential of -410 mV and (B) CV responses at different ethambutol concentrations for Au/PVP-Ag-PANSA/CYP2E1 biosensor (C) Ethambutol calibration curve of Au/PVP-Ag-PANSA/CYP2E1 biosensor with response time of 30 s.

The electrochemical Lineweaver-Burk equation (Equation 2) was used to evaluate K_M^{app} of the biosensor. In this case, the x-intercept of the graph represents $-1/K_m$ and the y-intercept is equivalent to the inverse of V_{max}.

$$\frac{1}{I_{ss}} = \frac{1}{I_{\max}} + \frac{K_m^{app}}{I_{\max}} \quad (4)$$

Here I_{ss} is the measured steady state current, I_{max} the maximum current under saturated substrate concentration, K_M^{app} the apparent Michaelis-Menten constant and [S] is the concentration of ethambutol. According to the intercept and slope of the above equation, the value for K_M^{app} was estimated to be 1,01 μM, whereas the value for the maximum I_{max} was calculated to be 0.65 μA. The K_M^{app} is lower than previously reported [37-40] for HRP immobilized in sol-gel-derived ceramic-carbon nanotubes composite film. The smaller value of K_M^{app} indicated for the present biosensor indicates that CYP2E1 embedded in the PANSA/ PVP-AgNPs nanocomposite has better affinity towards ethambutol and that this new electrode configuration is promising for building enzymatic devices with improved biocatalytic properties.

3.4. Stability and reproducibility of the modified electrode

The stability and reproducibility of the Au/PANSA/PVP-AgNPs/CYP2E1 electrode was also investigated. When the modified electrode was stored at 4 ^{0}C in 0.1 M, pH 7.4 phosphate buffer solution for two weeks, the current response retained more than 90 % of its original response. The relative standard deviation (R.S.D) was 3.2 % for ten successive measurements of 2 μM ethambutol, indicating excellent precision. The biosensor was used daily and stored in 0.1 M, pH 7.4 phosphate buffer solution at 4 ^{0}C when not in use. The data received from these experiments indicated that the current response only decreased by less than 10 % suggesting that the biosensor reported for this work has a long-term stability.

4. CONCLUSION

This study illustrated a simple strategy to obtain an efficient enzyme bioelectrochemical device based on a CYP2E1 modified Au electrode. The PANSA/PVP-AgNPs nanocomposite served as a suitable environment for enzyme attachment promoting the rapid catalytic conversion of ethambutol to ethambutol aldehyde facilitated by the transfer of electrons between the electrode surface and the enzyme active site. The efficiency of the sensor demonstrates that the peak ethambutol serum level which is 2 μg/mL (9.8 μM) is within the linear dynamic response range of 2-12 μM showing that this device can be used with success in serum. Chronoamperometry and CV were used to study the Michaelis-Menten region of the ethambutol responses where K_M^{app} and I_{max} where calculated to be 1,01 μM and 0.65 μA with a sensitivity of 1.13 μA/ μM and detection limit of 0.70 μM. The low

constant suggests that the modified electrode synthesis employed here is suitable for a novel enzymatic device with high biocatalytic activity preservation.

ACKNOWLEDGEMENTS
Financial assistance from the National Research Foundation of South Africa is greatly acknowledged.

References

1. L. Huang, T. Wen, *Mater. Chem .Phys.* 116 (2009) 474
2. M. R. Nabid, R. Dinarvand and R. Sedghi, *Int. J. Electrochem. Sci.* 3 (2008) 1117-1118
3. O.A. Sadik, S. K. Mwilu and A. Aluoch, *Electrochimca Acta*, 55 (2009) 4291-4292
4. T. Ahuja, D. Kumar, *Sensors and Actuators B* 136 (2009) 275-276
5. P. Norouzi, F. Faridbod, and M.R. Ganjali, *Int. J. Electrochem. Sci.* 5 (2010) 1214-1215
6. S. Reddy, B. E. Kumara Swamy, H. Jayadevappa, *Int. J. Electrochem Sci.* 5 (2010) 11
7. A. Alqudami, R. S. Rawat, *Synt. Met.* 157 (2007) 53-54
8. M. Li, G. Wang and B. Fang, *Anal. Biochem.*341 (2005) 52-53
9. O.A. Arotiba, B.B. Mamba and E. I. Iwuoha, *Int. J. Electrochem. Sci.* 6 (2011) 674
10. M. R. Guascito, D. Manno and A. Turco, *Biosens. Bioelectron.* 24 (2008) 1057-1058
11. I. Mickova, A. Prusi and L. Arsov, *Bulletin of the Chemists and Technologies of Macedonia* 25 (2006) 45-46
12. C. Liu, J. Hu, *Biosens. Bioelectron.* 24 (2009) 2149
13. S. Mu, Y. Qu and L. Jiang, *Colloid. Surf. A: Physiochemical and Engineering Aspects* 345 (2009)101-102
14. F. Cresphilho, S. A. Travains and O. N. Oliveira Jr, *Biosens. Bioelectron.* 24 (2009) 3073
15. J. Wang, *Biosens. Bioelectron.* 21 (2006) 1889-1891
16. J.H.O. Owino, O.A. Arotiba and R. F. Ngece, *Sensors* 8 (2008) 8263
17. E. Iwouha, R. Ngece and P. Baker, *IET Nanobiotechnology* 1 (2007) 62-64
18. N. Bistolas, U. Wollenberger and C. Jung, *Biosens. Bioelectron.* 20 (2005), 2409
19. S. Mu, C.Cheng and J. Wang, *Synt. Met.* 88 (1997), 249-254
20. L. Lin, P. Qiu, X. Cao and L. Jin, *Electrochima Acta* 53 (2008) 5370
21. L. Guo, Z. Peng and B. Tesche, *J. Colloid Interface Surf.* 319 (2008) 179-180
22. M. Li, G. Wang and B. Fang, *Anal. Biochem.* 341 (2005) 53-54
23. A. Salimi, S. Solranian, *Biophys. Chem.* 130 (2007) 124-125
24. C. Liu, J. Hu, *Biosens. Bioelectron.* 24 (2009) 2151-2152
25. S. Jing, C. Zhai, *Materials Letters* 61 (2007) 2796
26. M. Starowicz, B. Stypula and J. Banas, *Electrochem. Commun.* 8 (2009) 228-229
27. P. M. Cerqueira, F. H. Mateus and E.J. Evandro Jose´ Cesarino, *J. Chromatogr. B* 749 (2000) 153
28. S.Z. Zong, Y. Cao and H. X. Ju, *Electroanalysis* 19 (2007) 841-846
29. W.W. Yang, Y. C. Li and C.Q. Sun, *Sens. Actuators B: Chemistry* 115 (2006) 42-48
30. H. Zhang, N. F. Hu, *J. Phys. Chem. B* 111(2007) 10583-10590
31. L. Zang, X. Jiang, *Biosens. Bioelectron.* 213 (2005) 342-343.
32. E. Laviron, *J. Electrochem. Chem.* 100 (1979a), 263-270
33. E. Laviron, *J. Electrochem. Chem.*, 101 (1979b), 19-28
34. J. M. R. Perdeigão, R. Macedo and I. Portugal, *Int. J. Antimicrob. Agents* 33 (2009) 334
35. D. K. Spracklin, J.M. Fisher and E. D. Kharasch, *The Journal of Pharmacology and Experimental Therapeutic*, 281 (1997) 400 - 401
36. L.L. von Moltke , D.J. Greenbalt and S.X. Duan S.X, *Psychopharmacology* 132 (1997) 402-407
37. Y. Bai, H. Yang, W.Yang, Y. Li and C. Sun, *Sens. Actuators B: Chemistry* 124 (2007) 4179-4182

38. R. S. Costa, D. Machado, *Biosystems*, 100 (2010) 151
39. A. Cornish-Bowden, *Biochem. J.* 137 (1974) 143-174.
40. M. E.G. Lyons, *Int. J. Electrochem Sci.* 4 (2009) 80